Published in final edited form as:
Dev Dyn. 2011 October ; 240(10): 2245–2255. doi:10.1002/dvdy.22717.

Increased Expression of Syne1/Nesprin-1 Facilitates Nuclear Envelope Structure Changes in Embryonic Stem Cell Differentiation

Elizabeth R. Smith[1], **Xiao-Ying Zhang**[2], **Callinice D. Capo-chichi**[1], **Xiongwen Chen**[2], and **Xiang-Xi Xu**[1,+]

[1]Sylvester Comprehensive Cancer Center, Department of Medicine, and Department of Obstetrics and Gynecology, University of Miami School of Medicine, Miami, FL 33136

[2]Department of Physiology, Cardiovascular Research Center Temple University School of Medicine, Philadelphia, PA 19140

Abstract

We found by electron microscopy that the inter-membrane space of embryonic stem cells is irregular and generally wider than in differentiated cells. Among a panel of nuclear envelope structural proteins examined, the expression of Syne1/nesprin-1 was found to be greatly induced upon differentiation. Down regulation of Syne1 by siRNA in differentiated embryonic stem cells caused the nuclear envelope to adopt a configuration resembling that found in undifferentiated embryonic stem cells. Suppression of Syne1 expression did not produce a detectable impact on the retinoic acid-induced differentiation of embryonic stem cells; however, forced expression of Syne1 enhanced the tendency of the cells to lose pluripotency.

Thus, we found that low expression of Syne1 splicing isoforms accounts for the wider and irregular nuclear envelope inter-membrane space in embryonic stem cells. We conclude that the nuclear envelope structural change accompanying differentiation likely participates in promoting the differential chromatin organization of the differentiated cells.

Keywords

nuclear envelope; pluripotency; embryonic stem cells; mouse blastocysts

INTRODUCTION

The presence in cells of a compartmentalized unit, the nucleus, distinguishes eukaryotes from prokaryotes. The nucleus houses the genetic materials, the DNA, and ITS shell IS composeD of a double membrane of bi-layer lipids, known as the nuclear envelope. The outer nuclear envelope membrane integrates with the endoplasmic reticulum, and the inner membrane lies next to a layer of nuclear lamina, of which the main components include lamin, emerin, sun, and Synes/nesprins, and these basic features are conserved from worms and flies to mammals (Crisp and Burke, 2008; Gruenbaum et al., 2005; Gorjánácz et al., 2007). At least 80 unique integral membrane proteins of the nuclear envelope have been

[+]Corresponding author: Xiang-Xi (Michael) Xu, Ph.D., Professor of Medicine, Room 417 Papanicolaou Building, 1550 NW 10th Ave [M877], UM/Sylvester Comprehensive Cancer Center, Department of Medicine, Department of Obstetrics and Gynecology, University of Miami Miller School of Medicine, Miami, FL 33136, Tel: (305) 243-1750, xxu2@med.miami.edu.
ERS and XYZ made equal contribution to the work.
Present address for Xiao-Ying Zhang: Cardiovascular Research Center, Temple University, Philadelphia, PA 19140.

identified in mammalian cells (Schirmer et al., 2003). Many of these proteins interact directly or indirectly with lamins (Gruenbaum et al., 2005). Among these nuclear membrane proteins are three families, each of which is characterized by a distinct motif (specifically LEM, SUN, or KASH) (Wagner and Krohne, 2007). LEM-domain proteins (named after LAP2, emerin, and MAN1) interact with Baf (Segura-Totten and Wilson, 2004). Proteins that contain the SUN domain interact with partners containing the KASH (named after Klarsicht, ANC-1 and SYNE1 homology) domain (Tzur et al., 2006). In the mammalian nuclear envelope, known KASH domain containing proteins are the Syne (also known as nesprin) family proteins, and the Sun family proteins contain the Sun domain (Crisp et al., 2006; Worman and Gundersen, 2006; Zhang et al., 2001; Starr and Han, 2003). Both Syne1–3 and Sun1–3 are transmembrane proteins distributed in either inner or outer membrane of the nuclear envelope. The interaction between the KASH and SUN domains of proteins from the opposite membranes form bridges crossing the double nuclear envelope membranes (Worman and Gundersen, 2006; Warren et al., 2005).

Recent and ongoing studies are revealing the topology, localization in the inner or outer membranes, and biological function of many of these nuclear envelope components (Crisp and Burke, 2008). The double membrane structure is partially maintained by the presence of trans-membrane nuclear pore complexes distributed over the shell of the nuclear envelope (D'Angelo and Hetzer, 2008; Tran and Wente, 2006). Moreover, the bridges formed by the interaction between Sun1–3 and Syne1–3 in the peri-nuclear space also contribute to the structural organization of the nuclear envelope double membranes (Crisp et al., 2006). The inner membrane is tethered to the nuclear lamina through multiple molecular interactions, such as between emerin and lamin, and Lap and lamin (Gruenbaum et al., 2005). The nuclear envelope and lamina are then tethered to nucleic acid (DNA) through interactions of lamin and Baf to DNA/chromatins (Segura-Totten and Wilson, 2004).

The nuclear pore is composed of multiple protein subunits, the nucleoporins (D'Angelo and Hetzer, 2008; Tran and Wente, 2006). These proteins form a channel that spans between the inner and outer membranes and distributes all over the nuclear envelope. The nuclear pores are essential for the regulated exchange of substances between the nucleus and the cytoplasm, export of RNA, import of proteins, and cycling of signaling molecules (D'Angelo and Hetzer, 2008; Tran and Wente, 2006).

The inter-nuclear envelope membrane Syne-Sun bridges are called LINC complexes, for linking the nucleus and cytoplasm (Crisp et al., 2006). The Syne and Sun proteins were first identified in *C. elegans* and *Drosophila* to have a role in tethering nuclei to the cytoplasmic actin cytoskeleton (Starr and Han, 2002, 2003; Grady et al., 2005; Yu et al., 2006). The nuclear positioning role is conserved in mammals, and Syne and Sun proteins are found to play roles in nuclear positioning and migration, and their deletion affects nuclear positioning in multiple tissue types (Zhang et al., 2007; Lei et al., 2009; Zhang et al., 2009; Zhang et al., 2010).

Studies of model organisms such as *C. elegans* and *Drosophila*, gene knockouts in mice, and inherited diseases in humans have revealed the biological importance of the nuclear envelope (Crisp and Burke, 2008; Gruenbaum et al., 2005; Gorjánácz et al., 2007). The most obvious role of the nuclear envelope is as a physical barrier to separate the DNA from the cytoplasm in G1 and S phases. However, the nuclear envelope and lamina play important roles in the organization of chromatin and regulation of gene expression. Certain transcription factors such as c-fos and Rb are known to be sequestered to the nuclear lamina (Ivorra et al., 2006; Johnson et al., 2004; Melcon et al., 2006; Markiewicz et al., 2006). Heterochromatin, which is highly condensed and transcriptionally inactive, appears to have higher affinity to the lamina of the nuclear envelope and usually localizes to the nuclear

periphery adjacent to the nuclear lamina (Meshorer and Misteli, 2006). Hence in cell differentiation, a fundamental change in the nuclear envelope structure may initiate systematic reorganization of chromatins and the associated global changes in gene expression.

This is possible in the case of embryonic stem (ES) cell differentiation. The chromatin of ES cells has a unique "open" conformation and all genes are poised to be activated as a characteristic of the pluripotency of the cells (Meshorer and Misteli, 2006). The nuclear envelope structure of ES cells is unique, where the nucleus is more malleable and less rigid than differentiated cells (Pajerowski et al., 2007). An attractive idea is that a unique nuclear envelope structure of ES cells organizes chromatin in such a way to permit pluripotency (Meshorer and Misteli, 2006).

Here, we report that ES cells have wider and irregular nuclear envelope inter-membrane space, which is distinct from differentiated cells. We further determined that low Syne1 expression accounts for this unique nuclear envelope structure in ES cells.

RESULTS

Structural Change of Nuclear Envelope Associated with ES Cell Differentiation

Upon retinoic acid treatment for 4 days, the majority (>90%) of murine ES cells differentiate into extraembryonic endoderm-like cells, indicated by both morphological changes and expression of endoderm markers (Capo-Chichi et al., 2005). We used electron microscopy (EM) to characterize and compare the morphology of the cells prior to and after differentiation. As shown in Fig. 1A, the gross morphology of ES cells and differentiated cells are distinctive. Compared to undifferentiated ES cells, the differentiated, endoderm-like cells have a large number of cellular vacuoles and surface microvilla (Fig. 1A, indicated by "*"). The nucleus is also distinctive as shown at a higher magnification: the ES cells lack dark materials (presumably heterochromatin) around the nuclear periphery, which are present in all differentiated cells (Fig. 1B, arrow).

Little is known about the cell biology of ES cells relevant to the unique property of pluripotency. Presumably ES cells maintain pluripotency by keeping chromatin in a unique, "opened" conformation that is poised for transcription activation. Since the nuclear envelope is important in the control of chromatin organization and in regulation of signaling by modulating the shuttling of molecules between the nucleus and the cytoplasm, we examined the ultrastructure of the nuclear envelope in pluripotent ES cells compared to cells that were differentiated to endoderm-like cells with retinoic acid. EM shows that differentiation greatly altered the structure of nuclear envelope. Specifically, the inter-membrane space of the nuclear envelope is wider and the space is more irregular in ES cells, compared to a narrow and more uniform lining of the membrane in the differentiated cells (Fig. 1C). The width between the inner and outer nuclear envelope membranes (the perinuclear space) was measured to be 32–48 nm in pluripotent cells and 20–30 nm in differentiated endoderm cells. The inter-membrane space of several adult cell types was also examined for comparison, shown by an example of the nuclear envelope of a primary mouse ovarian surface epithelial cell (Fig. 1C). The adult cell types of both primary and cultured lines show a nuclear envelope inter-membrane space similar to that of the differentiated endoderm cells, suggesting the wider inter-membrane space is unique for the nuclear envelope of ES cells.

To determine if the observed widening of the inter-membrane space is a phenomenon that results from maintaining ES cells in culture or has relevance in vivo, we examined the nuclear envelope in mouse blastocysts by EM (Fig. 2). The E3.5 blastocysts harvested from timed-matings contain a layer of differentiated trophectoderm cells lining the blastocoel and

the cells of the inner cell mass (ICM). The cells of the ICM are composed of a randomly distributed mixture of differentiating primitive endoderm and pluripotent ES cells. The nuclear envelope inter-membrane space was measured in EM images of 4 blastocysts, as shown by a representative example (Fig. 2A), and a wide distribution of widths was found, ranging from 20 to 50 nm (Fig. 2B). When we examined individual cells, we found consistently that the differentiated trophectoderm cells located on the monolayer covering the blastocoel have a narrower nuclear envelope inter-membrane space (Figure 2A), and the cells with a wider nuclear envelope inter-membrane space unanimously locate within the interior of the ICM (Figure 2A). Thus, in vivo pluripotent ES cells have a distinctive nuclear envelope structure and the narrowing of the nuclear envelope inter-membrane space associates with differentiation.

No Significant Alteration of Nuclear Pore Density Associated with ES Cell Differentiation

In considering the molecular basis of the nuclear envelope alteration associated with ES cell differentiation, we examined the changes in nuclear pores and the Syne-Sun proteins, which are the two types of structures that form bridges between the two membranes. We reasoned that either changes in the number or the structural components of the two types of complexes might cause a change in the nuclear envelope structure and width of the inter-membrane space.

First, the pore complex proteins were compared between pluripotent and retinoic acid-differentiated ES cells (Fig. 3A). A monoclonal antibody, anti-NPC (Davis and Blobel, 1986; 1987), that recognizes multiple nucleoporin proteins, was used to examine protein levels by Western blot. ES cell differentiation did not change the protein levels of nucleoporins (Nup153, 98, 62, and 54 kd) (Fig. 3A), although the 54 kd protein recognized by the anti-pore antibody is noticeably absent upon cell differentiation. The number and density of the nucleopores was also assayed by confocal immunofluorescence microscopy (Fig. 3B). Some slight variation in the intensity of nuclear pore staining was observed in both pluripotent and differentiated cell populations; however, no consistent difference between pluripotent and different ES cells was detectable as shown by examples in Fig. 3B. Thus, we conclude that no significant change occurs in the intensity or number of nuclear pore complexes upon ES cell differentiation.

Expression of Nuclear Envelope Components Associated with ES Cell Differentiation

We then used real time, quantitative PCR (qRT-PCR) to measure the changes in components of the Syne-Sun bridges since antibodies are not available for all the isoforms (Fig. 4). The initial experiments revealed that among the common Syne and Sun isoforms, Syne1 mRNA exhibited the most dramatic increase upon ES cell differentiation (Fig. 4A). The primers used to amplify Synes locate in the KASH domain (Fig. 4B), which interacts with Sun protein at the nuclear envelope (Worman and Gundersen, 2006; Warren et al., 2005; Starr and Han, 2003). Syne1 is a trans-membrane protein composed of a variable number of spectrin repeats, and contains a conserved KASH domain at the C-terminal end next to the trans-membrane region (Zhang et al., 2001) (Fig. 4B). The N-terminal cytoplasmic or nucleoplasmic region of full length Syne1 (Syne1 giant) contains two actin-binding calponin homology domains, which are thought to make direct connections with the actin cytoskeleton (Starr and Han, 2003; Worman and Gundersen, 2006; Wilhelmsen et al., 2005; Stewart et al., 2007). The Syne1 gene produces several proteins lacking either the C-terminus or N-terminus by either differential splicing or alternative translation start sites (Fig. 4B) (Worman and Gundersen, 2006; Warren et al., 2005). Several oligo primers were designed to test the expression of these isoforms (arrows in Fig. 4B), and analysis indicated that the expression of KASH domain-containing isoforms of Syne1 increased 5- to 9-fold upon ES cell differentiation (Fig. 4C). These KASH domain-containing isoforms amplified

by primer pairs P3, P4, and P5 are capable of forming inter-membrane bridges with the Sun protein. However, expression of Syne1 isoforms containing the N-terminal portion of protein where the actin-binding calponin domain locates (amplified by primer pair P2) did not change upon differentiation (Fig. 4C). Thus, only the nuclear envelope-localized Syne1 isoforms appear to increase upon ES cell differentiation. We also determined the changes in expression of other common nuclear envelope components, and found that the mRNA level of lamin A/C, emerin, Man1, and Nurim increased upon ES cell differentiation (Fig. 4D). Presumably, these proteins also contribute to the refined structural organization of the nuclear envelope in differentiated cells.

Impact of Syne1 Suppression on Nuclear Envelope Structure

Using immunofluorescence microscopy, we confirmed that the Syne1 protein was increased upon differentiation of ES cells, concomitant with increased lamin A/C (Fig. 5A). We then tested by siRNA suppression to determine if the increased expression of KASH domain containing Syne1 isoforms accounts for the narrowing of the nuclear envelope inter-membrane space associated with ES cell differentiation. siRNA preparations from several oligo sequences targeting the region at or near the KASH domain were tested for their ability to reduce Syne1 expression. A set of siRNA was found particularly efficient to reduce Syne1 expression in retinoic acid-differentiated ES cells as assayed by immunofluorescence microscopy (Fig. 5A). The nuclear envelope inter-membrane space was determined using EM. In four experiments, a widening of the inter-membrane space was found in the Syne1 siRNA-treated, retinoic acid-differentiated ES cells as shown by examples (Fig. 5B). Quantization of the nuclear envelope lumen indicates that the width increases from a mean of 26 nm to 48 nm following siRNA treatment to down regulate Syne1, and the difference is statistically significant. Thus, we speculate that a low basal expression of Syne1 in pluripotent ES cells may account for the wider and irregular spacing between nuclear envelope membranes, and an increased expression of Syne1, as well as Syne1-interacting nuclear envelope structural proteins such as lamin A/C, emerin, Sun2, and perhaps others, contributes to the narrowing and structural changes of the nuclear envelope inter-membrane space upon differentiation of the ES cells. However, the ability of the Syne1overexpression to narrow nuclear envelope inter-membrane space has yet to be directly demonstrated.

Influence of Syne1 Expression on Cell Differentiation

Despite our repeated attempts, we did not observed an obvious and reproducible phenotype (such as differentiation) of ES cells transfected with siRNA to suppress Syne1. In our experiments of ES cells in cultures, no differences in cell morphology, growth, or differentiation of ES cells was detected when Syne1 was down-regulated and nuclear envelope inter-membrane space became wider and irregular. Thus, the biological consequence of suppressed Syne1 expression is subtle and the absence of Syne1 does not significantly affect ES cell function in culture. The results are perhaps not surprising since Syne1 gene knockout in mice does not limit early embryogenesis (Zhang et al., 2007; Puckelwartz et al., 2009; Zhang et al., 2010). Likely sufficient redundancy is in place for the function of Syne1 in nuclear envelope organization.

We also tested if forced expression of Syne1 can induce differentiation of ES cells. Transient transfection yielded around 20% of cells expressing mCherry-Syne1, with the expected nuclear envelope and cytoplasmic distribution as detected by mCherry fluorescence of the fusion protein. The expression of the fluorescent fusion protein was labile, and the signals became very weak or non-detectable by day 3. On days 1 and 2 post transfection, the cells were subjected to analysis for immunofluorescence and fluorescence microscopy, and we determined that mCherry-Syne1 had no definite impact on the

expression of pluripotency marker Oct-3/4 (Niwa et al., 2000) or endoderm marker GATA4 (Capo-chichi et al., 2005). Syne1 expression construct without mCherry fusion was also tested to ensure Syne and mCherry-Syne1 have the same activity.

We also tested whether Syne1 expression offers potentiating activity for ES cell differentiation by culturing the ES cells in the presence of 0.01 μM retinoic acid (RA). The low concentration of RA by itself has no significant impact on the pluripotency and differentiation of the ES cells. As a control, transfection of histone H2B constructs into ES cells treated with 0.01 μM RA did not change the expression of Oct3/4 that are expressed by the majority (90%) of ES cells (Fig. 6A, B). Strikingly, in the presence of low RA as a potentiating agent, the majority of mCherry-Syne1 expressing cells lost the expression of Oct3/4, a marker of pluripotency of embryonic stem cells (Niwa et al., 2000) (Fig. 6C, D). The inverse correlative expression between mCherry-Syne1 and Oct3/4 was shown by examples in Fig. 6C (arrows), and the quantitation is illustrated in Fig. 6D. In three separate transfections, more than 90% of mCherry-Syne1 expressing cells cultured in the presence of 0.01 μM RA were found to be Oct3/4 negative (Fig. 6C, D). Only a small percentage of mCherry-Syne1 expressing cells still exhibited a diminishing Oct3/4 expression, as shown in examples in Fig. 6C (arrowhead). Thus, forced expression of Syne1 promotes the loss of pluripotency and induces differentiation in ES cells in the presence of low concentration of retinoic acid as a potentiating agent.

In the same experiments, we also tested if forced expression of Syne1 induces the expression of GATA4, a marker for primitive endoderm (Capo-chichi et al., 2005). GATA4 was absent in many mCherry-Syne1 expressing cells even in the presence of 0.01 μM RA (Fig. 6E, arrow). Examination of multiple fields of cells indicated that more than 80% of mCherry expressing cells lacked GATA4 expression (Fig. 6F). The 10–20% of GATA4 expressing cells is similar to the percentage (5–10%) of cells undergoing spontaneous endoderm differentiation in the presence of low concentration of RA. We conclude that in the presence of a potentiating agent (low concentration of RA), forced expression of Syne1 promotes embryonic stem cells differentiation (or loss of pluripotency), but does not particularly incline differentiation towards the primitive endoderm lineage.

DISCUSSION

We observed that pluripotent ES cells possess a unique nuclear envelope structure: a wider perinuclear space than differentiated cells. The distance between the inner and outer nuclear envelope membranes may be determined by two types of connections between the membranes, the nuclear pore and the Nesprin/Syne-Sun bridges. Compared to differentiated cells, the pluripotent ES cells have low expression of several nuclear envelope structure proteins, and the increase in Syne1 seems to be most dramatic. By suppressing Syne1 expression in the differentiated ES cells, a widening of the internuclear envelope membrane space was observed. Thus, we conclude that increased Syne1 expression is the key factor accounting for the narrowing of the perinuclear space associated with ES cell differentiation.

The Syne1 isoforms found to increase upon ES cell differentiation are the smaller and KASH domain containing, but not the full length or the actin-binding calponin domain containing spliced isoforms. Current data suggests that these smaller isoforms (Nesprin 1alpha and 2 beta) locate in the inner membrane and present inside nucleus (Mislow et al., 2002; Zhang et al., 2001). Presumably, the width of the lumen does not depend on the large Syne1 isoforms. In that case, the KASH domain of these Syne1 isoforms forms construct bridges spanning the lumen with Sun proteins that locate on the outer nuclear envelope membrane.

The distinctive nuclear envelope structure of ES cells most likely plays a role in presenting certain aspects of the pluripotent cell type. One possibility is that the unique nuclear envelope structure of the pluripotent ES cells is to accommodate the unique “poised” chromatin organization of the cells (Meshorer and Misteli, 2006). The ES cells have little heterochromatin material, and an increased presence of heterochromatin shows as dark material around the inner nuclear envelope in differentiated cells. We have so far not yet uncovered an obvious phenotype of ES cells transfected with siRNA to suppress Syne1, and Syne1 suppression does not significantly alter ES cell differentiation induced by retinoic acid. Similarly, manipulating the expression of lamin A that is increased upon ES cell differentiation, was reported not to affect the differentiation of embryonic carcinoma cells (Peter and Nigg, 1991). Thus, the lack of lamin A/C expression in pluripotent ES cells (Röber et al., 1989) may account for the physical plasticity of the cells (Pajerowski et al., 2007), but a role in the cellular function of the ES cells has not yet been defined.

Syne1 is not essential for early embryogenesis since Syne1 C-terminal deletion mutant mice die at or near birth from respiratory failure, whereas surviving mice display hindlimb weakness and an abnormal gait (Zhang et al., 2007; Puckelwartz et al., 2009; Zhang et al., 2010). The findings at the cellular level also suggest that Syne1 participates in a complex that links the nucleoskeleton to the cytoskeleton (Starr and Han, 2002, 2003; Crisp et al., 2006; Wilhelmsen et al., 2005; Libotte et al., 2005; Padmakumar et al., 2005). In cultured rat hippocampal neurons, it was reported that some Syne1 isoforms participate in endocytic internalization of synaptic proteins (Cottrell et al., 2004). In agreement with the non-essential function of Syne1 in early development (Zhang et al., 2007; Puckelwartz et al., 2009; Zhang et al., 2010), we did not observe any significant effects when Syne1 is suppressed in differentiating ES cells. Likely, redundancy from other Syne family members or functionally overlapping proteins masked the role of Syne1 in the ES cell differentiation culture system and in vivo. Although Syne1 appears to be non-essential for differentiating ES cells, a low Syne1 protein level, possibly in conjunction with expression of other nuclear envelope proteins (such as low lamin A/C), may be important for the organization of chromatin and maintenance of the pluripotent state of ES cells.

We found that forced expression of Syne1 by itself is not sufficient to induce the differentiation of ES cells in culture. However, in the presence of a low concentration of RA as potentiating agent, which does not impact ES cell differentiation by itself, expression of Syne1 is able to induce the loss of Oct3/4, a marker of ES cell pluripotency. However, forced expression of Syne1 appears not to bias differentiation into extraembryonic lineage (GATA4 as a marker), which is the primary lineage of differentiation of ES cells in culture. These results support a model (Meshorer and Misteli, 2006) in which coordinated changes in the expression of Syne1 and other nuclear envelope proteins impact pluripotency and stages of differentiation by differential organization of chromatins.

In sum, we observed a distinctive nuclear envelope structure in pluripotent ES cells and suggest that this wider inter-membrane space can be accounted for by low Syne1 expression in ES cells. We speculate that the unique nuclear envelope structure of the ES cells may have a role in organizing chromatins of pluripotent state that are poised to activate and attribute to all developmental lineages. Thus, the study suggests that nuclear envelope structure has a determining role in the differentiation of embryonic stem cells.

MATERIALS and METHODS

Embryonic Stem Cell Cultures

Lines of RW-4 and W-4 mouse embryonic stem cells obtained from Fox Chase Cancer Center tissue culture facility were maintained in ES medium with LIF on a layer of

irradiated mouse embryonic fibroblasts as previously described (Capo-Chichi et al., 2005). The ES cells were treated with 1 μM retinoic acid (RA) for 4–6 days to induce endoderm differentiation as described previously (Capo-Chichi et al., 2005). The degree of differentiation was confirmed by expression of endoderm markers Dab2 and GATA4 using immunofluorescence microscopy.

For experiments in potentiating the differentiation of ES cells, 0.01 μM RA was included in culture medium a day prior to transfection. This low concentration of RA induced insignificant differentiation, but promotes the impact of Syne1 expression on the pluripotency and differentiation of ES cells.

Histology, Immunostaining, Immunofluorescence Microscopy, and General Laboratory Procedures

Standard H&E, immunohistochemical staining, and Western blotting were performed as detailed previously (Capo-Chichi et al., 2005; Yang et al., 2005). The sources of antibodies were: Mouse monoclonal anti-NPC Proteins (hybridoma 414 that recognizes several proteins in the nuclear pore complex of various species) (Davis and Blobel, 1986; 1987), Sigma, Inc.; Mouse anti-lamin A/C antibodies, and goat anti-Nesprin1/Syne1, Santa Cruz Biotechnology, Inc. (Santa Cruz, CA); Mouse monoclonal anti-importin B1, Affinity Bioreagents; Goat polyclonal anti-importin 7, Imgenex.

Generally, cells were cultured on glass coverslips or on chamber slides and analyzed using CCD or laser-scanning confocal microscopy. DAPI was used as a nuclear marker. Immunofluorescence staining was described in detail previously (Capo-Chichi et al., 2005; Yang et al., 2005). Nikon Eclipse E 800 epifluorescence microscope with 60X oil immersion objective linked to a Roper Quantix CCD (charged coupled device) camera and a Zeiss Axio Observer Z1 with a 63X oil immersion objective were used to examine the slides. A Nikon Eclipse E800 fluorescence microscope with 60X water immersion objective linked to a Bio-Rad Radiance 2000 LSCM (laser scanning confocal microscope) camera was also used for observation and image acquisition.

Electron Microscopy

To culture ES cells free from MEFs, cells were first cultured on an uncoated petri dish for 45 min, and cells that did not attach were collected and further cultured on a new uncoated Petri dish for another 45 min. Cells not attached were then collected and grown on glass coverslips coated with 0.1% gelatin in ES cell culture medium, and were differentiated into primitive endoderm cells by treating with 1 μM RA for 6 days. Undifferentiated cells were grown on coverslips in ES cell medium without RA. Mouse ovarian surface epithelial cells (MOSE) were isolated from mouse ovaries and cells were grown on glass coverslips. Day E3.5 blastocysts were collected and attached onto coverslips coated with poly-L-lysine.

Fixation and embedding of tissues followed by ultrathin sectioning and staining were carried out according to a standardized method. Briefly, ES or MOSE cells growing on coverslips or blastocysts attached onto poly-L-lysine coated coverslips, were fixed with 2% glutaraldehyde/2% formaldehyde in 0.1 M cacodylate, pH 7.0, for 30 min at room temperature; the fixative was changed and the samples were further fixed on ice with 2% glutaraldehyde/2% formaldehyde for 60 min. Samples were then washed 3 times with 0.1 M cacodylate, followed by three washes with distilled water. Samples were post-fixed for 30 min with 2% uranyl acetate, washed 5 times with distilled water, and post-fixed for 60 min with 1% osmium tetroxide. After dehydration, the cells or tissues were embedded in Epon. Coverslips were cleaned from the bottom as much as possible with hydrofluoric acid. For undifferentiated or differentiated ES cells, colonies of cells with distinctive undifferentiated

or differentiated features were selected under the microscope before ultrathin sectioning. Ultrathin sections of ~80 nm in thickness were stained for 5 min with 2% uranyl acetate dissolved in 70% ethanol, and for 2 min with lead citrate prepared using Reynolds' method. The sections were observed in an electron microscope (JEM-1210) using an acceleration voltage of 80 kV. The nuclear surface was observed at a magnification of 49,000X.

Measurement of Inter-membrane Distance

EM images were captured and stored as digital data and analyzed using NIH Image J software. Images with the nuclear envelope cut perpendicularly to the nuclear surface were chosen for quantitation of perinuclear space. A strip of image encompassing the nuclear envelope was scanned at the cross section at 90-degree angle (perpendicular) to quantify electron density range on a 256 gray scale.

For selection of images of the nuclear envelopes cut perpendicularly to the nuclear surface, the following criteria were adopted from a published study (Matsubara and Kitaguchi, 2004): 1) the perinuclear cistern was clearly observed; 2) the outer nuclear membrane was seen as a line with thickness of less than 10 nm.

Expression and siRNA Suppression of Syne1

The Syne1/Nesprin-1 cDNA construct in pCMV-SPORT6 plasmid (I.M.A.G.E. Clone ID: 6492523; GenBank Number: BC054456; from *Mus musculus* retina) was obtained from ATCC. The Syne1 coding sequence was first cloned into pAcGFP1-N1 by replacing the GFP coding sequence (through SalI/NotI sites). This construct is predicted to express untagged Syne1. The mCherry coding sequence was then inserted in-frame with the N-terminus of Syne1 to avoid possible interference of mCherry with the Syne1 KASH domain in the C-terminus. The second construct is predicted to express a mCherry-Syne1 fusion protein. These constructs have been fully verified by sequencing. Transfection of plasmid DNA expression constructs into ES cells was performed using Lipofectamine 2000, following the manufacturer's protocol for ES cells.

A mixture of oligos for siRNA targeting Syne1/nesprin-1 was purchased from Santa Cruz Biotech. The oligos were transfected into ES cells according to the manufacturer's protocol. Cells were analyzed 72 hours following transfection.

Quantitative Real-Time PCR (qRT-PCR)

Total RNA was isolated using the Qiagen RNAeasy kit from undifferentiated ES W-4 cells or those differentiated into primitive endoderm cells by treating with RA for 6 days.

Nuclear envelope proteins including Syne1/nesprin-1, Syne2/nesprin-2, Syne3/nesprin-3, Sun1, Sun2, Sun3, BAF, emerin, lamin A/C, lamin C, lamin B1, lamin B2, lamin B receptor, LAP1, LAP2, Man1, HP1α, β, γ, LEM2, LEM3, Nurim, along with housekeeping genes (actin, hprt, tbp, rpst, tftr, tubb3), were analyzed by real-time PCR. Expression of nuclear envelope proteins at the mRNA level was normalized to hprt (which shows very little variation between ES cells and differentiated cells). Taqman probe/primer sets were purchased from Applied Biosystems if available; otherwise, self-designed primer pairs were used together with SYBR green. The location of the primer pairs is indicated in Figure 4B and the sequences are listed in the Supplemental Table 1. Expression of nuclear envelope proteins at the mRNA level was normalized to hprt, which shows very little variation between differentiated and undifferentiated ES cells.

Supplementary Material

Refer to Web version on PubMed Central for supplementary material.

Acknowledgments

We acknowledge the excellent technical assistance from Jennifer Smedberg and Malgorzata Rula. We thank Dr. Robert Moore for his assistance in harvesting blastocysts and ES cell culturing and thank Dr. Kathy Q. Cai and Ying Wang for technical advice and suggestions for immunofluorescence microscopy in the experiments. These experiments were initiated at the Fox Chase Cancer Center (Philadelphia, PA) and completed at the University of Miami (Miami, FL) following relocation of the Xu lab. We appreciate the assistance and contribution of Dr. Michal Jarnik of the Fox Chase Cancer Center Imaging Facility, Xiang Hua of the Fox Chase Cancer Center Transgenic Mouse Facility, Tony Lerro and Jackie Valvardi of the Fox Chase Cancer Center Animal Facility, Sharon Howard from the Cell Culture Facility, Dr. Emmanuel Nicolas of the Fannie E. Rippel Biochemistry and Biotechnology Facility, Cass Renner and Fangping Chen of the Fox Chase Cancer Center Pathology Facility. These studies were supported by funds from grants R01 CA095071, CA79716 and CA75389 to X.X. Xu from NCI, NIH.

References

Capo-Chichi CD, Rula ME, Smedberg JL, Vanderveer L, Parmacek MS, Morrisey EE, Godwin AK, Xu XX. Perception of differentiation cues by GATA factors in primitive endoderm lineage determination of mouse embryonic stem cells. Dev Biol. 2005; 286:574–586. [PubMed: 16162334]

Cottrell JR, Borok E, Horvath TL, Nedivi E. CPG2: a brain- and synapse-specific protein that regulates the endocytosis of glutamine receptors. Neuron. 2004; 44:677–690. [PubMed: 15541315]

Crisp M, Liu Q, Roux K, Rattner JB, Shanahan C, Burke B, Stahl PD, Hodzic D. Coupling of the nucleus and cytoplasm: role of the LINC complex. J Cell Biol. 2006; 172:41–53. [PubMed: 16380439]

Crisp M, Burke B. The nuclear envelope as an integrator of nuclear and cytoplasmic architecture. FEBS Lett. 2008; 582:2023–2032. [PubMed: 18474238]

Davis LI, Blobel G. Identification and characterization of a nuclear pore complex protein. Cell. 1986; 45:699–709. [PubMed: 3518946]

Davis LI, Blobel G. Nuclear pore complex contains a family of glycoproteins that includes p62: glycosylation through a previously unidentified cellular pathway. Proc Natl Acad Sci USA. 1987; 84:7552–7556. [PubMed: 3313397]

D'Angelo MA, Hetzer MW. Structure, dynamics and function of nuclear pore complexes. Trends Cell Biol. 2008; 18:456–466. [PubMed: 18786826]

Gorjánácz M, Jaedicke A, Mattaj IW. What can Caenorhabditis elegans tell us about the nuclear envelope? FEBS Lett. 2007; 581:2794–2801. [PubMed: 17418822]

Grady RM, Starr DA, Ackerman GL, Sanes JR, Han M. Syne proteins anchor muscle nuclei at the neuromuscular junction. Proc Natl Acad Sci U S A. 2005; 102:4359–4364. [PubMed: 15749817]

Gruenbaum Y, Margalit A, Goldman RD, Shumaker DK, Wilson KL. The nuclear lamina comes of age. Nat Rev Mol Cell Biol. 2005; 6:21–31. [PubMed: 15688064]

Ivorra C, Kubicek M, González JM, Sanz-González SM, Alvarez-Barrientos A, O'Connor JE, Burke B, Andrés V. A mechanism of AP-1 suppression through interaction of c-Fos with lamin A/C. Genes Dev. 2006; 20:307–320. Erratum in: 2006 Genes Dev 20, 747. [PubMed: 16452503]

Johnson BR, Nitta RT, Frock RL, Mounkes L, Barbie DA, Stewart CL, Harlow E, Kennedy BK. A-type lamins regulate retinoblastoma protein function by promoting subnuclear localization and preventing proteasomal degradation. Proc Natl Acad Sci USA. 2004; 101:9677–9682. [PubMed: 15210943]

Lei K, Zhang X, Ding X, Guo X, Chen M, Zhu B, Xu T, Zhuang Y, Xu R, Han M. SUN1 and SUN2 play critical but partially redundant roles in anchoring nuclei in skeletal muscle cells in mice. Proc Natl Acad Sci U S A. 2009; 106:10207–10212. [PubMed: 19509342]

Libotte T, Zaim H, Abraham S, Padmakumar VC, Schneider M, Lu W, Munck M, Hutchison C, Wehnert M, Fahrenkrog B, Sauder U, Aebi U, Noegel AA, Karakesisoglou I. Lamin A/C-dependent localization of Nesprin-2, a giant scaffolder at the nuclear envelope. Mol Biol Cell. 2005; 16:3411–3424. [PubMed: 15843432]

Markiewicz E, Tilgner K, Barker N, van de Wetering M, Clevers H, Dorobek M, Hausmanowa-Petrusewicz I, Ramaekers FC, Broers JL, Blankesteijn WM, Salpingidou G, Wilson RG, Ellis JA, Hutchison CJ. The inner nuclear membrane protein emerin regulates beta-catenin activity by restricting its accumulation in the nucleus. EMBO J. 2006; 25:3275–3285. [PubMed: 16858403]

Matsubara S, Kitaguchi T. Pathological changes of the myonuclear fibrous lamina and internal nuclear membrane in two cases of autosomal dominant limb-girdle muscular dystrophy with atrioventricular conduction disturbance (LGMD1B). Acta Neuropathol. 2004; 107:111–118. [PubMed: 14673599]

Melcon G, Kozlov S, Cutler DA, Sullivan T, Hernandez L, Zhao P, Mitchell S, Nader G, Bakay M, Rottman JN, Hoffman EP, Stewart CL. Loss of emerin at the nuclear envelope disrupts the Rb1/E2F and MyoD pathways during muscle regeneration. Hum Mol Genet. 2006; 15:637–651. [PubMed: 16403804]

Meshorer E, Misteli T. Chromatin in pluripotent embryonic stem cells and differentiation. Nat Rev Mol Cell Biol. 2006; 7:540–546. [PubMed: 16723974]

Mislow JM, Holaska JM, Kim MS, Lee KK, Segura-Totten M, Wilson KL, McNally EM. Nesprin-1alpha self-associates and binds directly to emerin and lamin A in vitro. FEBS Lett. 2002; 525:135–140. [PubMed: 12163176]

Niwa H, Miyazaki J, Smith AG. Quantitative expression of Oct-3/4 defines differentiation, dedifferentiation or self-renewal of ES cells. Nat Genet. 2000; 24:372–376. [PubMed: 10742100]

Padmakumar VC, Libotte T, Lu W, Zaim H, Abraham S, Noegel AA, Gotzmann J, Foisner R, Karakesisoglou I. The inner nuclear membrane protein Sun1 mediates the anchorage of Nesprin-2 to the nuclear envelope. J Cell Sci. 2005; 118:3419–3430. [PubMed: 16079285]

Pajerowski JD, Dahl KN, Zhong FL, Sammak PJ, Discher DE. Physical plasticity of the nucleus in stem cell differentiation. Proc Natl Acad Sci USA. 2007; 104:15619–15624. [PubMed: 17893336]

Peter M, Nigg EA. Ectopic expression of an A-type lamin does not interfere with differentiation of lamin A-negative embryonal carcinoma cells. J Cell Sci. 1991; 100:589–598. [PubMed: 1808207]

Puckelwartz MJ, Kessler E, Zhang Y, Hodzic D, Randles KN, Morris G, Earley JU, Hadhazy M, Holaska JM, Mewborn SK, Pytel P, McNally EM. Disruption of nesprin-1 produces an Emery Dreifuss muscular dystrophy-like phenotype in mice. Hum Mol Genet. 2009; 18:607–620. [PubMed: 19008300]

Röber RA, Weber K, Osborn M. Differential timing of nuclear lamin A/C expression in the various organs of the mouse embryo and the young animal: a developmental study. Development. 1989; 105:365–378. [PubMed: 2680424]

Schirmer EC, Florens L, Guan T, Yates JR 3rd, Gerace L. Nuclear membrane proteins with potential disease links found by subtractive proteomics. Science. 2003; 301:1380–1382. [PubMed: 12958361]

Segura-Totten M, Wilson KL. BAF: roles in chromatin, nuclear structure and retrovirus integration. Trends Cell Biol. 2004; 14:261–266. [PubMed: 15130582]

Starr DA, Han M. Role of ANC-1 in tethering nuclei to the actin cytoskeleton. Science. 2002; 298:406–409. [PubMed: 12169658]

Starr DA, Han M. ANChors away: an actin based mechanism of nuclear positioning. J Cell Sci. 2003; 116:211–216. [PubMed: 12482907]

Stewart CL, Roux KJ, Burke B. Blurring the boundary: the nuclear envelope extends its reach. Science. 2007; 318:1408–1412. [PubMed: 18048680]

Tran EJ, Wente SR. Dynamic nuclear pore complexes: life on the edge. Cell. 2006; 125:1041–1053. [PubMed: 16777596]

Tzur YB, Wilson KL, Gruenbaum Y. SUN-domain proteins: 'Velcro' that links the nucleoskeleton to the cytoskeleton. Nat Rev Mol Cell Biol. 2006; 7:782–788. [PubMed: 16926857]

Wagner N, Krohne G. LEM-Domain proteins: new insights into lamin-interacting proteins. Int Rev Cytol. 2007; 261:1–46. [PubMed: 17560279]

Warren DT, Zhang Q, Weissberg PL, Shanahan CM. Nesprins: intracellular scaffolds that maintain cell architecture and coordinate cell function? Expert Rev Mol Med. 2005; 7:1–15. [PubMed: 15953398]

Wilhelmsen K, Litjens SH, Kuikman I, Tshimbalanga N, Janssen H, van den Bout I, Raymond K, Sonnenberg A. Nesprin-3, a novel outer nuclear membrane protein, associates with the cytoskeletal linker protein plectin. J Cell Biol. 2005; 171:799–810. [PubMed: 16330710]

Worman HJ, Gundersen GG. Here come the SUNs: a nucleocytoskeletal missing link. Trends Cell Biol. 2006; 16:67–69. [PubMed: 16406617]

Yang DH, Cai KQ, Roland IH, Smith ER, Xu XX. Disabled-2 is an epithelial surface positioning gene. J Biol Chem. 2007; 282:13114–13122. [PubMed: 17339320]

Yu J, Lei K, Zhou M, Craft CM, Xu G, Xu T, Zhuang Y, Xu R, Han M. KASH protein Syne-2/Nesprin-2 and SUN proteins SUN1/2 mediate nuclear migration during mammalian retinal development. Hum Mol Genet. 2011; 20:1061–1073. [PubMed: 21177258]

Yu J, Starr DA, Wu X, Parkhurst SM, Zhuang Y, Xu T, Xu R, Han M. The KASH domain protein MSP-300 plays an essential role in nuclear anchoring during Drosophila oogenesis. Dev Biol. 2006; 289:336–345. [PubMed: 16337624]

Zhang Q, Skepper JN, Yang F, Davies JD, Hegyi L, Roberts RG, Weissberg PL, Ellis JA, Shanahan CM. Nesprins: a novel family of spectrin-repeat-containing proteins that localize to the nuclear membrane in multiple tissues. J Cell Sci. 2001; 114:4485–4498. [PubMed: 11792814]

Zhang J, Felder A, Liu Y, Guo LT, Lange S, Dalton ND, Gu Y, Peterson KL, Mizisin AP, Shelton GD, Lieber RL, Chen J. Nesprin 1 is critical for nuclear positioning and anchorage. Hum Mol Genet. 2010; 19:329–341. [PubMed: 19864491]

Zhang X, Xu R, Zhu B, Yang X, Ding X, Duan S, Xu T, Zhuang Y, Han M. Syne-1 and Syne-2 play crucial roles in myonuclear anchorage and motor neuron innervation. Development. 2007; 134:901–908. [PubMed: 17267447]

Zhang X, Lei K, Yuan X, Wu X, Zhuang Y, Xu T, Xu R, Han M. SUN1/2 and Syne/Nesprin-1/2 complexes connect centrosome to the nucleus during neurogenesis and neuronal migration in mice. Neuron. 2009; 64:173–187. [PubMed: 19874786]

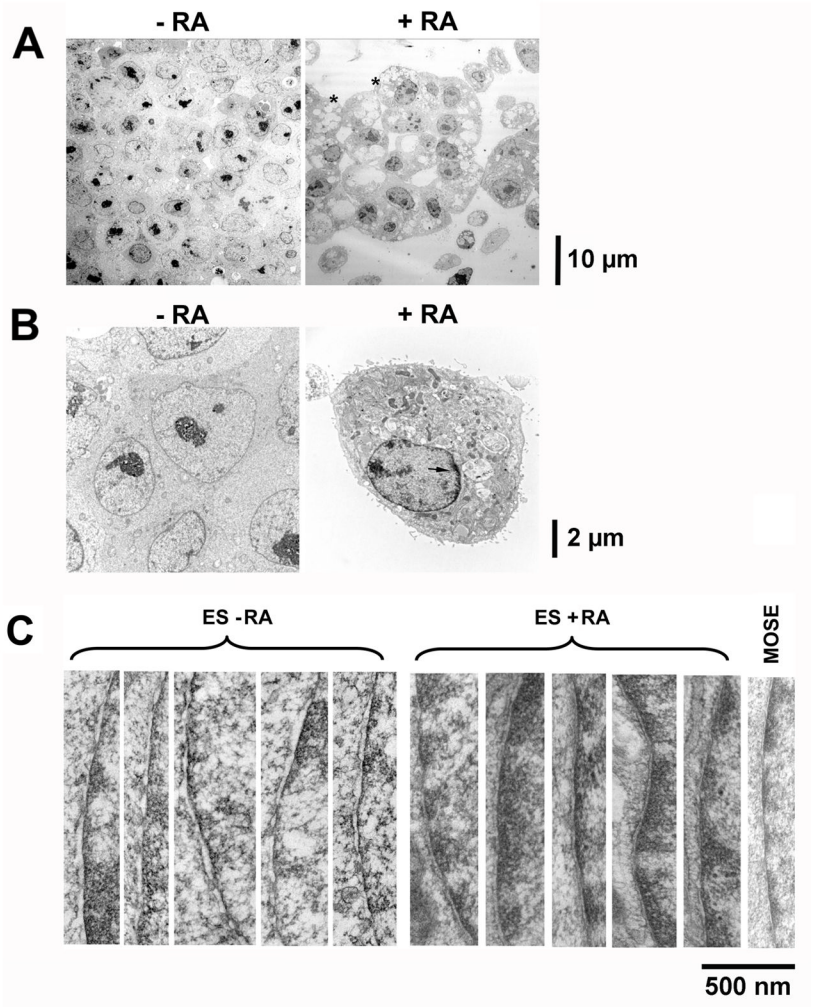

Figure 1. Characterization of mouse embryonic stem cells by EM

Mouse ES cells free of MEF feeder were cultured without or with retinoic acid (1 μM) for 6 days to induce differentiation, and the cells were processed for EM analysis. (**A**) Low magnification (2070X at 7-inch print) EM views of mouse ES cells compared to differentiated ES cells. The presence of cellular vacuoles and surface microvilla in the differentiated cells is indicated by "*". (**B**) Higher magnification (8280X at 7-inch print) of representative undifferentiated and differentiated ES cells. The heterochromatin indicated by the dark material at the nuclear periphery is shown by an arrow. (**C**) High magnification (84500X at 7-inch print) images focusing on segments of nuclear envelope were obtained and 5 each of representative images were shown for undifferentiated and differentiated ES cells. An image of a nuclear envelope from mouse ovarian surface epithelial cells is shown for comparison. Scale bars next to the images indicate size.

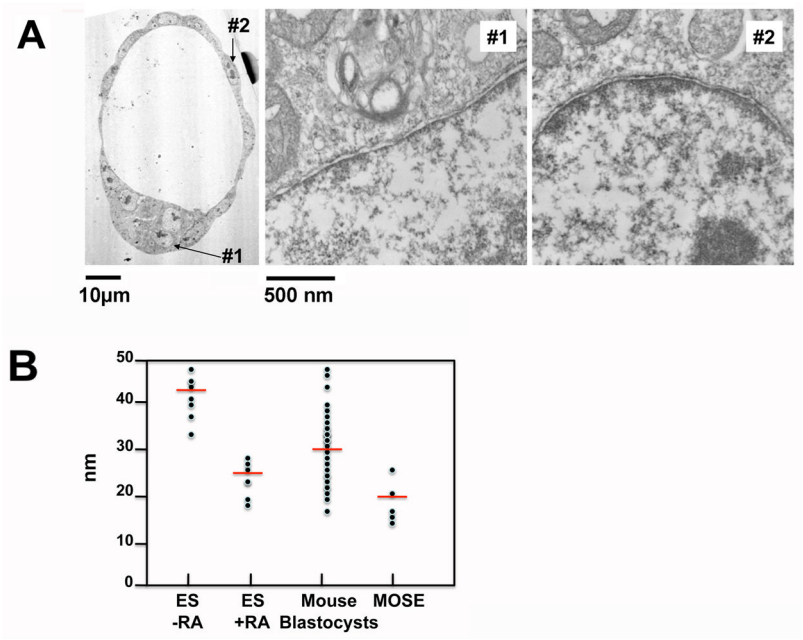

Figure 2. Characterization of mouse blastocysts by EM

Mouse blastocysts at around E3.5 stage were harvested and processed for analysis by EM. The experiments were repeated twice with 10 independently isolated blastocysts each and representative images are presented. (**A**) Low magnification (2070X at 7-inch print) EM views of a mouse blastocyst. The high magnification (84500X at 7-inch print) EM images of a segment of nuclear envelope of indicated cells (#1, inner cell mass; and #2, trophectoderm cell) are shown. Scale bars are included to indicate size. (**B**) Quantitation by measurement of inter-membrane space of the nuclear envelopes. The pluripotent ES cells, differentiated ES cells, blastocysts, and mouse ovarian surface epithelial cells were subjected to EM analysis. The peri-nuclear space was estimated from multiple cells for comparison. The differences in nuclear envelope lumen space between differentiated and undifferentiated ES cells were statistical significant ($p < 0.0001$) as determined by Student's T-test.

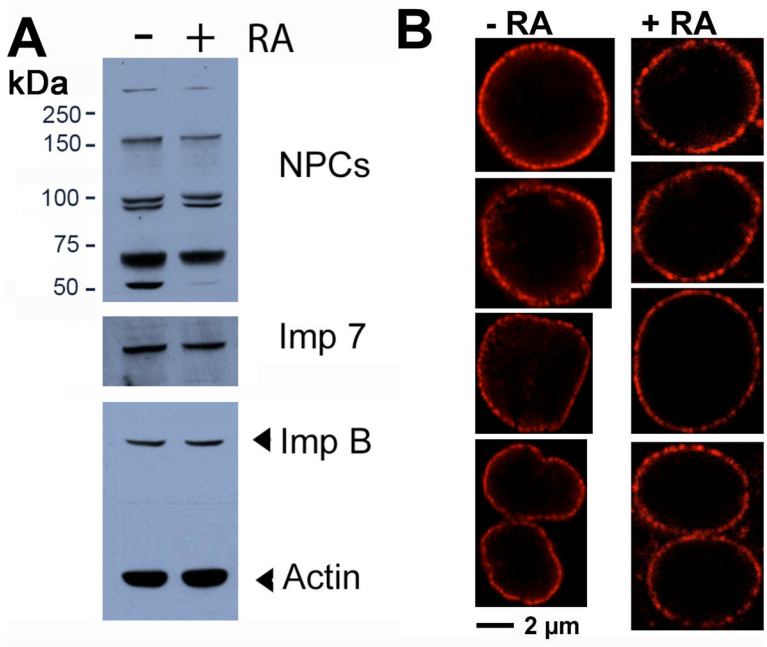

Figure 3. Analysis of nuclear pore complexes of undifferentiated and retinoic acid-differentiated ES cells

(**A**) Cultured mouse ES cells and their differentiated derivatives following retinoic acid treatment for 6 days were harvested for Western blotting of components of nuclear pore complexes using anti-pore antibodies. Importin 7 (Imp 7) and importin beta (Imp B) were also determined. Beta-actin was used as a loading control. (**B**) Confocal microscopy images of nuclear pore staining using the anti-NPC antibodies are shown for pluripotent and retinoic acid-differentiated ES cells. Four representative images each are shown for comparison.

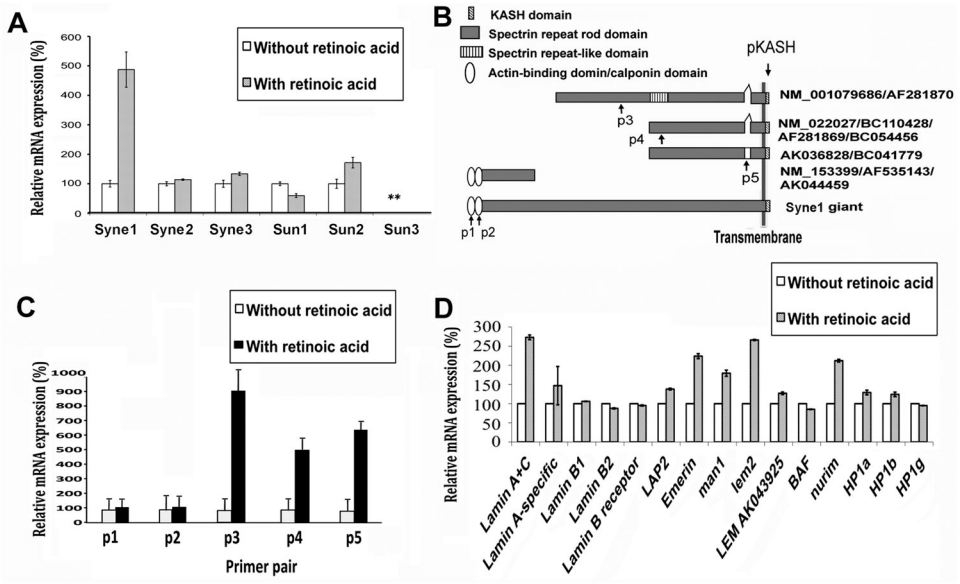

Figure 4. Quantitative RT-PCR analysis of nuclear envelope components in undifferentiated and retinoic acid-differentiated ES cells

Cultured mouse ES cells and their differentiated derivatives following retinoic acid treatment for 4 days were harvested for expression analysis by qRT-PCR of a panel of nuclear envelope components. (**A**) Syne and Sun isoforms were analyzed for their expression by qRT-PCR. For Synes, the primer sequences locate in the KASH domain (pKASH). Relative expression levels are shown by normalizing the expression as “100%” in undifferentiated cells. “**”, the expression level of Sun3 is too low for analysis. The increase in Syne1 expression upon cell differentiation is statistically significant ($p < 0.005$). (**B**) The structural isoforms of Syne1 are illustrated. The GENBANK assession numbers and the location of primers used in PCR are shown. (**C**) Syne1 isoforms were further analyzed by qRT-PCR using specific primer pairs (p1–5). The location of the primer pairs is indicated in (**B**) and the sequences are listed in Supplemental Table 1. (**D**) Additional nuclear envelope proteins as well as HP1alpha, beta, and gamma were analyzed by quantitative RT-PCR. The expression of several putative housekeeping genes was also measured and serves as controls (not shown). Expression of nuclear envelope proteins at the mRNA level was normalized to hprt (which shows very little variation between ES cells and differentiated cells). Expression levels are shown by normalizing the expression as “100%” in undifferentiated cells.

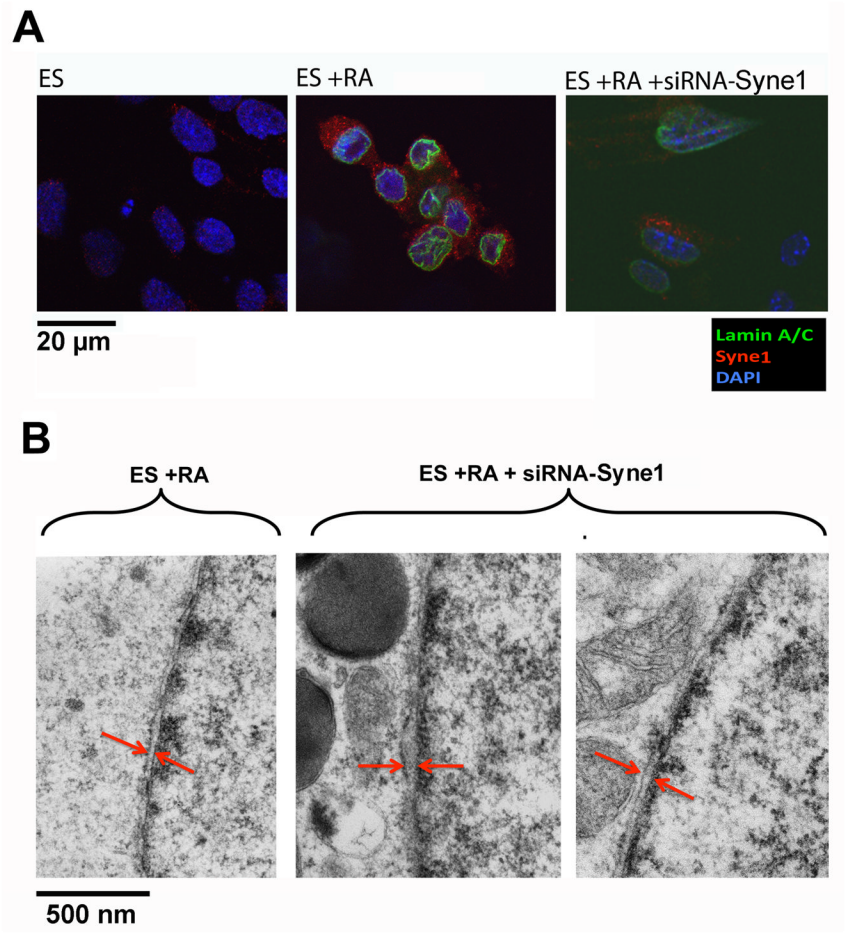

Figure 5. Effects of siRNA Syne1 suppression on the nuclear envelope structure of ES cells

Cultured mouse embryonic stem cells and their differentiated derivatives following retinoic acid treatment for 4 days were treated with siRNA to Syne1. (**A**) Immunofluorescence microscopy was performed for Lamin A/C (green), Syne1 (red), and Dapi (blue) compared to undifferentiated ES cells, differentiated ES cells, and differentiated ES cells treated with siRNA to Syne1. (**B**) The cells were processed for EM analysis of nuclear envelope inter-membrane space. Twenty cells each were analyzed and an example of differentiated ES cells and two examples of siRNA-Syne1 treated differentiated ES cells are shown (84500X at 7-inch print). The differences in nuclear envelope lumen space between differentiated ES cells and those treated with siRNA were statistical significant ($p < 0.0001$) as determined by Student's T-test, with a mean of 26 nm and 48 nm respectively.

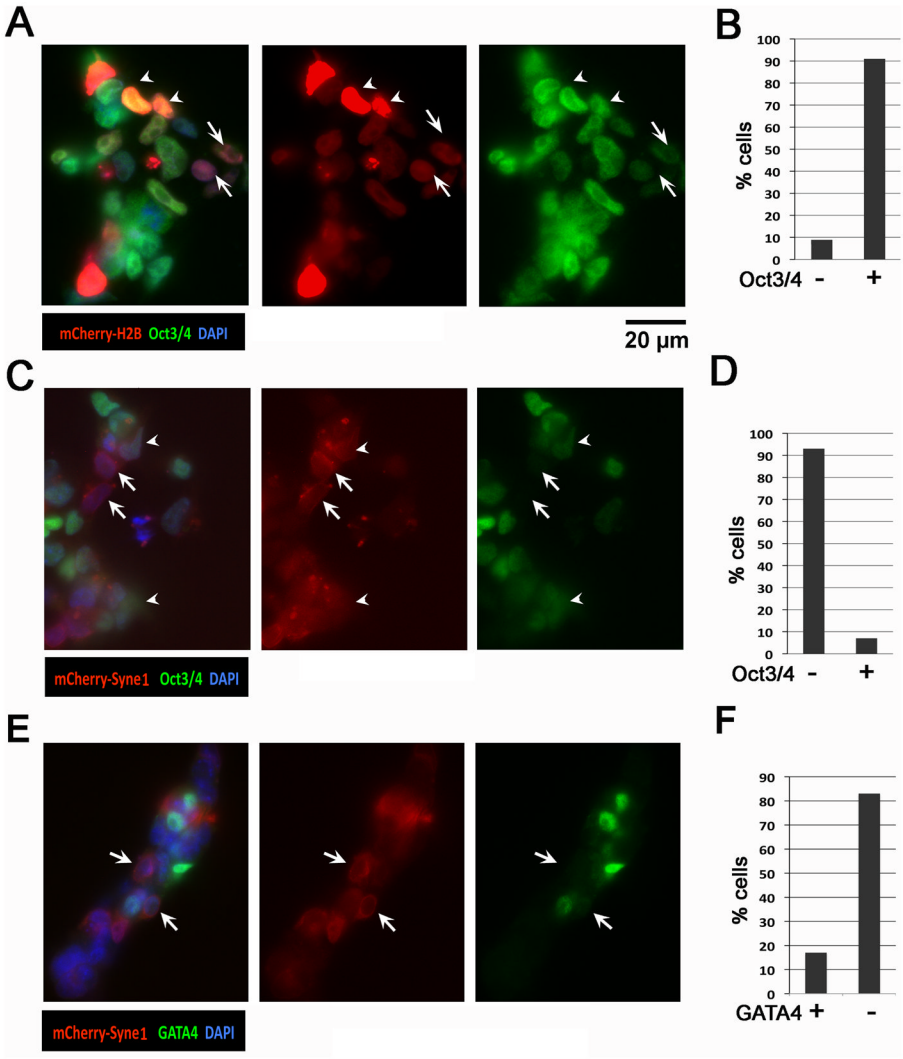

Figure 6. Forced expression of Syne1 on pluripotency and differentiation of ES cells

ES cells were transfected with control vector, Syne1 expression vector, mCherry-histone H2B expression construct (as a control), and mCherry-Syne1 fusion protein expression construct. Following incubation of the ES cells with DNA vector using Lipofectamine 2000 for 5 hours, the cells were changed to fresh medium with 0.01 μM RA. After 24 to 48 hours, the cells were washed with PBS and subjected for analysis with fluorescence and immunofluorescence microscopy. (**A**) The ES cells transfected with mCherry-histone H2B expression construct were analyzed for the expression of mCherry-histone H2B (red) and immunofluorescence of Oct-3/4 (green). DAPI staining (blue) was used to mark nuclei. Arrowhead indicates examples of mCherry-histone H2B and Oct3/4 positive cells. Arrow indicates examples of mCherry-histone H2B positive cells with a reduced Oct3/4 expression. (**B**) mCherry-histone H2B positive cells were quantified as Oct-3/4 positive and negative. A total of 50 plus mCherry-histone H2B positive cells were quantified from 10 acquired images. (**C**) The ES cells were analyzed for the expression of mCherry-Syne1 (red) and immunofluorescence of Oct3/4 (green). DAPI staining (blue) was used to mark nuclei. Arrowhead indicates examples of mCherry-Syne1-positive cells with a reduced Oct3/4 expression. Arrow indicates examples of mCherry-Syne1-positive cells with no Oct3/4 expression. (**D**) mCherry-Syne1 positive cells were quantified as Oct3/4 positive and

negative. A total of 50 plus mCherry-Syne1 positive cells were quantified from 10 acquired images. (**E**) The ES cells were analyzed under fluorescence microscopy for the expression of mCherry-Syne1 (red) and immunofluorescence of GATA4 (green). DAPI staining (blue) was used to mark nuclei. Arrow indicates examples of mCherry-Syne1-positive cells with no GATA4 expression. (**F**) mCherry-Syne1 positive cells were quantified as GATA4 positive and negative. A total of over 50 mCherry-Syne1 positive cells were quantified from 10 acquired images. These experiments have been repeatedat least five times with similar and reproducible results.